Article ID: 1006-8775(2017) 03-0334-11

INTEGRATED RISK ASSESSMENT OF MAJOR METEOROLOGICAL DISASTERS WITH PAPRIKA PEPPER IN HAINAN PROVINCE

ZHANG Lei (张 蕾)[1, 3], HUO Zhi-guo (霍治国)[1, 2], ZHANG Li-zhen (张立祯)[4], HUANG Da-peng (黄大鹏)[5]

(1. Chinese Academy of Meteorological Sciences, Beijing 100081 China;
2. Collaborative Innovation Center on Forecast and Evaluation of Meteorological Disasters, Nanjing University of Information Science & Technology, Nanjing 210044 China; 3. National Meteorological Center, Beijing 100081 China;
4. China Agricultural University, Beijing 100083 China; 5. National Climate Center, Beijing 100081 China)

Abstract: Paprika pepper, as one of the main vegetable crops, is originated in the tropics and now widely planted in the world for its dietary therapy and medicinal functions. For its typical physiological properties referring to low tolerances to flood, drought and cold, paprika pepper often suffers from one or several disasters during its growing period, especially under tropical climate. Paprika pepper in Hainan, as a typical region of tropical climate in China, sustains flood, chilling and drought disaster risks induced by varied weather systems. This study was to develop and employ appropriate indices to assess hazard, sensitivity, vulnerability and prevention capability for major disasters during paprika pepper growth period, using long-term meteorological data from 1998 to 2011, actual disasters record from 1999 to 2011, production and socioeconomic statistics from 2002 to 2011 at 18 weather stations. Based on the Analytic Hierarchy Process and Entropy method, the combined weight was given to each disaster factor, thus an integrated disaster risk assessment model was developed and applied at regional level. High flood hazard mainly occurred in eastern Hainan, high chilling hazard in north and central mountain areas, and high drought hazard in the western part of Hainan. Drought and chilling sensitivity had a similar spatial distribution which decreased from central to coastal regions while flood sensitivity was the opposite. High vulnerability of the disasters mainly occurred in central regions, similar to low prevention capability. Eastern Hainan suffered from high integrated damage risk. The predicted damage occurrence showed a good agreement with the occurrence of actual disasters. We concluded that an integrated damage risk assessment model could provide a new tool to assess major meteorological disasters and help farmers and policy makers to alleviate the risks of major meteorological disasters for paprika pepper, which seems also suitable for other crops.

Key words: flood; chilling; drought; integrated risk assessment; paprika pepper
CLC number: S42 **Document code:** A
doi: 10.16555/j.1006-8775.2017.03.010

1 INTRODUCTION

Meteorological disasters cause enormous economic loss, taking up about 38% of total production in the world and more than 15% in China during the period from 1900 to 2014 (Emergency Events Database [1]). Resulting from climate change, an increasing trend was found in intensity and frequency of meteorological disasters (Zhang et al.[2]), which damaged 5 billion ha of crops per year with the loss of economic values as high as 200 billion Chinese Yuan per year in the whole of China (Jia et al.[3]).

Paprika pepper, as one of the important vegetable crops with high contents of vitamin C, E and protein, originates in tropical Latin America and widely grows in many countries in Asia, Africa, Europe, South and North America. Paprika pepper is mainly produced in warm and sunny climate in the southern area of China. As a ‘winter vegetable basket’ of China, Hainan province has unique climatic advantage and topographic environment. As a major vegetable crop, paprika pepper developed quickly since 1980s, accounting for almost 30% of total vegetables at present in Hainan. Owing to various weather systems interaction, meteorological disasters such as rainstorms, floods, droughts and chilling severely threaten paprika pepper production. For example, about 0.41 million ha of vegetable crops were damaged by droughts in the spring of 2005, and 0.14 million ha by the flood in October 2010. 20% to 30% of vegetable yields were lost due to chilling conditions in the winter of 2008. It is therefore imperative to assess the disaster risk in vegetable production to help farmers optimize their crops by minimizing disaster losses.

Received 2016-04-12; **Revised** 2017-07-27; **Accepted** 2017-08-15

Foundation item: Meteorological Public Welfare Profession of China (GYHY201206019); Basic Scientific Research Fund of CAMS (2015Y003); National Science and Technology Basic Project of China (2007FY120100)

Biography: ZHANG Lei, Ph. D., Research Assistant, primarily undertaking research on climate change and agrometeorology.

Corresponding author: HUO Zhi-guo, e-mail: huozhigg@cam-scma.cn

Risk assessment of meteorological disasters is to quantify the hazard, sensitivity, vulnerability and prevention capability of disasters by developing and applying various assessment measures. A lot of studies have been done to assess the impact and risk of meteorological disasters on agriculture at the field level (Luedeling et al.[4]; Aghdam and Mohammadkhani[5]; Bi et al. [6]) and at the regional level by using different spatial-temporal scales (Deo [7]; Varazanashvili et al.[8]; Glade and Nadim[9]; IPCC[10]). Using an appropriate index in the assessment of disaster risk is the pivotal issue, however, the current indices are very different and difficult to apply in paprika pepper because several disasters often occurred simultaneously. Drought probabilities for precipitation (Petr et al.[11]), soil electric conductivity (Delin and Berglund[12]) and surface runoff (Quan et al. [13]) were used to assess drought and flood risk. Indices e.g. period of precipitation (Zhang[14]) and consecutive rainless days (Xu et al.[15]) were also used to assess the drought risk without taking account of actual damages. Indices derived from water supply and demand, e.g. relative severity index (Todisco et al.[16]), standardized precipitation index (Yu et al. [17]), palmer drought severity index (Dash et al. [18]), multi-scale standardized precipitation index (Potopová et al. [19]), reconnaissance drought index (Tsakiris et al.[20]), drought vulnerability index (Shahid and Behrawan [21]), daily composite drought index (Li et al.[22]) and standardized precipitation evapotranspiration index (Vera et al. [23]), are often used and reasonable results are obtained. However, these indices are calculated based on numerous data sheets and difficult to parameterize. To assess chilling risk, the indices are generally grouped into two categories: (a) average cold temperature without considering crop chilling requirement like consecutive cold days (Liu et al. [24]), and (b) crop biological characteristics-based indices depend on biological minimum temperature (Megias et al.[25]), i.e. relative accumulated chilling (Rebecca et al. [26]) and weighted cumulated degree days (Giulia et al.[27]).

With the development of GIS and RS technologies, some indices have been derived for extending disasters analysis (Cheng et al.[28]), with a temperature condition index (Belal et al.[29]) based on the information of land surface temperature versus NDVI scatter plots falling into a triangular shape, a water supplying vegetation index defined as the ratio of the fourth channel brightness temperature of NOAA AVHR to NDVI, and a vegetation condition index based on the status of vegetation cover as a function of NDVI minima and maxima (Sanjay et al.[30]). However, the vegetation data is not easy to be precisely monitored. It is therefore necessary for a scientific and simple index for single and multiple disasters to be developed and applied to specific vegetable crops addressing their specialties and the meteorological disasters they suffer from.

Most often than not, there is more than one disaster occurring in one crop growing season, however, we have limited knowledge to assess multiple disasters by using one simple and practical measure. Our objectives were to (1) develop appropriate indices for the assessment of hazard, sensitivity, vulnerability and prevention capability for each single disaster, i.e. flood, chilling and drought for paprika pepper; (2) integrate indices of each single disaster into a combined assessment model to assess the risk of overall major meteorological disasters; and (3) apply the integrated risk assessment model in paprika pepper production in Hainan, China, and generally compare the results of the assessment with the actual severity of meteorological disasters in the studied region.

2 MATERIALS AND METHODS

2.1 *Study area and data source*

The current study was performed in Hainan Island in the north of South China Sea (18°10'N–20°10'N, 108°37'E–111°03'E), the second largest island in China with a total area of 34 ha (Wen and Wu[31]). The climate of the studied region is tropical. Yearly mean air temperature ranges from 22.8 to 26.7 ℃, total rainfall per year is from 960 to 2,500 mm, and yearly sunshine duration varies from 1,800 to 2,811 h.

Paprika pepper in the studied region was sown in September and harvested during April and May. During the growing season of paprika pepper, flood, chilling and drought occurred singly or jointly. Three periods corresponding to the development stages of paprika pepper, i.e., October to November in the preceding year in the seedling stage, preceding December to February during vegetative growth, and March to April during flowering, were analyzed. The data included meteorological data, disaster damage records, production data and socioeconomic statistical data. Daily meteorological data including mean and minimum air temperatures and precipitation from 1998 to 2011 at 18 weather stations near the studied sites (Fig.1) were obtained from Institute of Meteorological Science of Hainan Province. To ensure the coherence of records, individual missing climate data (less than 5%) of weather stations were replaced by mean values of the same time during 1998–2011.

Disaster damage data were extracted from Chinese Meteorological Disasters Service (Wen and Wu[31]) and from Institute of Meteorological Science of Hainan Province from 1998 to 2011. Production data of paprika pepper from 1999 to 2011, i.e., yield and planting area, were obtained from Vegetables Institute of Hainan Academy of Agricultural Sciences. Socioeconomic statistical data (net income per capita in rural areas and agricultural machinery gross power) were extracted from Hainan Agricultural Statistics Yearbook from 2002 to 2011. Digital Elevation Model (DEM) was used in topographic analysis (Masood and Takeuchi [32]) for the distribution of the disasters. The DEM data of Hainan

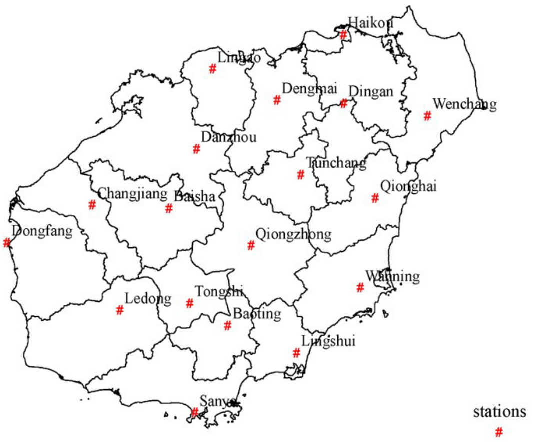

Figure 1. Distribution of 18 studied sites and weather stations in Hainan province, China.

province were obtained from Institute of Meteorological Science of Hainan Province.

2.2 *Assessing the risks of major disasters*

Risk assessment was a complex process that depends on comprehensive analysis of various climatic, ecological, social and economical variables. First, we developed models to assess the single index for hazard, sensitivity, vulnerability and prevention capability for each meteorological disaster, i.e., flood, chilling and drought. Then, we developed an integrated damage risk assessment model to assess the overall disasters risk for paprika pepper by combining all indices and disasters.

2.2.1 DISASTER HAZARD

Flood and drought disaster were directly caused by water content deviating from precipitation. Four factors, i.e. amount of precipitation, dry days, continuous dry days and maximum continuous dry days were selected to characterize the drought. The amount of precipitation, rain days, continuous rain days and maximum continuous rain days were used for flood. Significant correlation between every two of the four selected factors for flood and drought at each station was at first analyzed. Secondly, the principal component analysis (PCA) method was used to select most important factors, when the accumulative contribution rate of the first two principal components accounted for more than 88% and 85% (Table 1), respectively. Thirdly, a linear combined index of the first two principal components multiplying by each contribution rate was taken as a drought or flood hazard index, which was a non-dimensional index by using standardized factors.

Table 1. Correlation coefficients between every two factors and accumulative contribution rate of the first two principal components of the four factors for flood and drought at each station.

Station	Correlation coefficient of factors												Accumulative contribution rate (%)	
	Drought						Flood							
	*$C_{P,DD}$	$C_{P,CD}$	$C_{P,MD}$	$C_{DD,CD}$	$C_{DD,MD}$	$C_{CD,MD}$	$C_{P,RD}$	$C_{P,CR}$	$C_{P,MR}$	$C_{RD,CR}$	$C_{RD,MR}$	$C_{CR,MR}$	**Fl	***Dr
Haikou	−0.51	−0.43	−0.08	0.94	0.59	0.62	0.58	0.57	0.41	0.99	0.69	0.70	90.46	89.91
Dongfang	−0.40	−0.38	−0.23	0.99	0.57	0.52	0.55	0.50	0.08	0.96	0.46	0.48	88.26	85.50
Danzhou	−0.39	−0.37	−0.10	0.99	0.60	0.57	0.55	0.57	0.79	0.98	0.60	0.63	94.48	88.39
Qiongzhong	−0.46	−0.43	−0.14	0.97	0.47	0.48	0.69	0.64	0.72	0.99	0.83	0.81	94.58	85.60
Qionghai	−0.68	−0.60	−0.35	0.98	0.56	0.60	0.55	0.64	0.68	0.98	0.86	0.83	95.11	89.71
Sanya	−0.46	−0.37	−0.46	0.98	0.68	0.69	0.54	0.51	0.49	0.97	0.61	0.69	88.24	89.88
Lingshui	−0.53	−0.49	−0.41	0.98	0.84	0.81	0.45	0.46	0.76	0.97	0.67	0.70	94.57	94.08
Dingan	−0.59	−0.56	−0.23	0.97	0.33	0.27	0.59	0.61	0.45	0.98	0.77	0.81	93.31	85.83
Lingao	−0.57	−0.56	−0.35	0.98	0.51	0.44	0.52	0.49	0.70	0.97	0.61	0.52	92.03	85.72
Dengmai	−0.57	−0.50	−0.56	0.95	0.45	0.48	0.56	0.54	0.65	0.99	0.70	0.67	91.79	87.90
Changjiang	−0.27	−0.25	−0.38	0.98	0.54	0.44	0.66	0.67	0.41	0.97	0.58	0.58	89.25	85.95
Wenchang	−0.86	−0.84	−0.15	0.97	0.28	0.24	0.37	0.43	0.40	0.99	0.77	0.82	93.10	94.73
Wanning	−0.67	−0.63	−0.35	0.97	0.56	0.64	0.55	0.59	0.76	0.99	0.83	0.83	96.38	90.23
Tunchang	−0.65	−0.56	−0.21	0.97	0.58	0.55	0.50	0.56	0.88	0.99	0.51	0.52	96.72	90.44
Baisha	−0.67	−0.60	−0.43	0.96	0.56	0.53	0.46	0.53	0.82	0.99	0.64	0.72	96.09	87.72
Ledong	−0.28	−0.27	0.44	0.98	0.28	0.30	0.46	0.47	0.45	0.97	0.75	0.82	92.48	90.38
Baoting	−0.60	−0.52	−0.11	0.97	0.66	0.63	0.43	0.49	0.41	0.97	0.75	0.78	91.80	92.92
Tongshi	−0.64	−0.57	−0.11	0.99	0.64	0.70	0.56	0.53	0.56	0.99	0.58	0.58	88.78	95.09

Note: *$C_{P,DD}$ indicates the correlation coefficient between precipitation (P) and dry days (DD). Similarly, CD indicates continuous dry days, MD maximum continuous dry days for drought. $C_{P,RD}$ indicates the correlation coefficient between precipitation (P) and rain days (RD), CR indicates continuous rain days and MR indicates maximum continuous rain days for flood. **Fl=flood; ***Dr=drought.

According to physiological characteristics of paprika pepper, the plant suffered from chilling damage when the daily air minimum temperature is lower than 12℃ (Cheng[33]). By the analysis of the continuous days with temperature below 12℃ of each chilling event based on historical record, we found that for every obvious chilling event, for example the typical chilling years in 2000 and 2008, there existed at least one period that was more than five continuous days with minimal air temperature below a minimum chilling temperature (T_c, 12℃). Therefore, we used two parameters, i.e. T_c and at least last 5 days, to assess the chilling hazard. The accumulated chilling, when the chilling event lasted more than 5 days, was calculated by Eq.1.

$$X = 0.25\sum_{n=1}^{m}(T_c - T_{min})^2/(T_{mean} - T_{min}) \qquad (1)$$

where X is the accumulated chilling, T_{min} is the daily minimum air temperature, T_{mean} is the daily mean air temperature, and T_c is the threshold temperature of chilling with a value of 12℃.

The disaster hazard (H) assessment model for drought, flood or chilling was built based on the grade of each hazard and risk probability (Eq.2).

$$H = \sum_{i=1}^{n} J_i \times P_i \qquad (2)$$

where J_i is hazard intensity referring to the mean value of hazard index for all flood, chilling or drought disasters at level i respectively. Here, i is divided into three levels: 1 for light, 2 for moderate and 3 for high damage. P_i is risk probability at a level i calculated by soft histogram estimation (Wu et al.[34]). Hazard level for each disaster was classified by hazard index, which was calculated from the value of 20%–50%, 50%–80% and above 80% of an ordered series of hazard index value of historical disasters damage. The hazard index for flood ranged from 0.50 to 2.65. When the hazard index ranged from 0.50 to 1.30, based on the above percentage of the ordered series calculated from historical records, we characterized the hazard level as 1 (light), when it was from 1.30 to 1.80, we set it as level 2 (moderate) and when it was from 1.80 to 2.65, we made it level 3 (high). For chilling hazard with the chilling index ranging from 1 to 27.2℃·d, level 1 was from 1 to 5℃·d, level 2 from 5 to 10℃·d and level 3 from 10 to 27.2℃·d. The range of drought index for drought ranged from −2.12 to 0.5, for level 1 from −0.15 to 0.5, level 2 from −0.70 to −0.15 and level 3 from −2.12 to −0.70. The levels 1, 2 and 3 of disaster hazard referred to high, medium and low hazard, respectively that was classified by natural breaks method with the ArcGIS 9.3 software.

2.2.2 DISASTER SENSITIVITY

Sensitivity of disasters, defined as the probability of hazard-affected body prone to disaster, was largely determined by regional terrain and topographic environment(Ozsahin and Kaymaz[35]). Flood was affected by the slope gradient, which was sensitive to small terrain slope gradient where water easily gathers around, while drought was sensitive to large one. With the altitude increasing, chilling sensitivity tended to increase due to decreasing temperatures. The terrain slope gradient and its reciprocal factor were selected as sensitivity indices (S) for drought and flood separately calculated by the Slope module on ArcGIS 9.3 (Environmental Systems Research Institute, America) using the widely used DEM data. Sensitivity index (S) for chilling was calculated by the sea level elevation through normalization of DEM data on ArcGIS 9.3.

2.2.3 DISASTER VLNERABILITY

Vulnerability of each disaster (V) was defined as the product of the yield reduction rate (y) and the risk probability of disasters (f) (Eq.3). The yield reduction rate was computed by actual yield (y_i) and tendency yield (y_t) (Eq.4). The tendency yield was computed by the method of straight line moving average(Ruiz et al.[36]).

$$V = \sum_{i=1}^{n} y_i \times f_i \qquad (3)$$

$$y = \frac{y_i - y_t}{y_t} \times 100\% \qquad (4)$$

where y_i is the average yield reduction rate at grade i from 1 to 3. The grade 1 refers to a yield reduction rate of 5% to 10%, 10% to 20% for grade 2 and above 20% for grade 3. f_i is risk probability at grade i, which is calculated by soft histogram estimation method (Wu et al.[34]).

2.2.4 DISASTER PREVENTION CAPABILITY

Disaster prevention capability (P) was defined as the production stability affected by agricultural and economic factors (h) in relation to the contribution weight (w) by each of the factors (Eq.5). The agricultural factors were the variation coefficient of yield, slope of regression between tendency yield and proportion of paprika pepper plant area over total area of vegetables. The economic factors were the net income per capita in rural area and agricultural machinery gross power. These five factors could generally reflect the regional agriculture and economic stability.

$$P = \sum_{i=1}^{m} h_i \times w_i \qquad (5)$$

where h_i is the prevention capability for each factor i. w_i is the corresponding weight, which is determined by a combination weighted average of Analytic Hierarchy Process method (w_{ia}) (Nasiri et al.[37]) and Entropy method (w_{ie}) (Benedetto et al.[38]). w_{ia} represents a subjective weight while w_{ie} represent an objective one. The calculated weights of w_{ia}, w_{ie} and w_i are listed in Table 2.

$$w_i = \frac{w_{ia} \times w_{ie}}{\sum_{i=1}^{5} w_{ia} \times w_{ie}} \times 100\% \qquad (6)$$

Among the five factors of disaster prevention

Table 2. The weights of five agricultural and economic factors determining the prevention capability against disasters.

Agricultural and economic factor	$*w_{ia}$	$*w_{ie}$	$*w_i$
Variation coefficient of yield	0.528	0.162	0.449
Slope of the regression for tendency yield	0.217	0.251	0.287
Proportion of paprika pepper plant area	0.089	0.234	0.109
Net income per capita in rural area	0.083	0.179	0.078
Agricultural machinery gross power	0.083	0.174	0.076

Note: $*w_{ia}$ indicates a weight derived from Analytic Hierarchy Process method and w_{ie} is derived from Entropy method. w_i is an integrated weight of w_{ia} and w_{ie}.

capability, the variation coefficient of yield area ratio had the highest w_{ia} while the slope of regression of tendency yield had the highest w_{ie}. The integrated weight wi for the variation coefficient of yield was higher (0.449) than that for the slope of regression of tendency yield (0.287), proportion of paprika pepper plant area (0.109), net income per capita in rural area (0.078) and agricultural machinery gross power (0.076).

2.2.5 INTEGRATED RISK ASSESSMENT MODEL FOR THREE MAJOR DISASTERS

To assess the overall meteorological disaster risk in paprika pepper, an integrated risk (F) model was developed based on the indices of hazard(H), sensitivity (S), vulnerability (V) and prevention capability (P) of three major disasters.

$$F=\left(\sum_{j=1}^{3} a_j H_j^{w_{hj}} \times S_j^{w_{sj}}\right)^{w_d} \times V^{w_v} \times \left(\frac{1}{P^{w_p}}\right) \tag{7}$$

where H_j is the hazard index of disaster j. S_j is the sensitivity index of disaster j. j indicates the disaster of flood, chilling or drought separately, i.e. flood=1, chilling=2 and drought=3. V is the vulnerability index. P is the prevention capability index. w_{hj} is the weight of hazard for disaster j, and w_{sj} is the weight for sensitivity. a_j is the weight of the hazard and sensitivity for disaster j. w_d, w_v and w_p are the weight for hazard and sensitivity, vulnerabilities, prevention capabilities of all disasters, respectively. As listed in Table 3, w_{hj} , w_{sj}, a_j, w_d, w_v and w_p are the corresponding weights given by a combination weight on average with the Analytic Hierarchy Process method and Entropy method mentioned in Eq. 6.

The combined weights for each disaster in the integrated model are listed in Table 3. The combination weight of flood (a_1) was the highest (0.733) in hazard and sensitivity, followed by drought (a_3) and chilling (a_2). Disaster hazard and sensitivity had the highest combination weight (w_d) in the integrated damage risk model, which indicated that hazard and sensitivity played more important role than vulnerability (w_v) and disaster prevention capability (w_p).

Table 3. The weight of comprehensive damage risk assessment factors.

Factor	Weight	Factor	Weight	Factor	Weight
Flood hazard (w_{h1})	0.620	Flood hazard and sensitivity (a_1)	0.733	Disaster hazard and sensitivity (w_d)	0.585
Flood sensitivity (w_{s1})	0.103				
Chilling hazard (w_{h2})	0.069	Chilling hazard and sensitivity (a_2)	0.083		
Chilling sensitivity (w_{s2})	0.014				
Hazard (w_{h3})	0.161	Drought hazard and sensitivity (a_3)	0.193		
Drought sensitivity (w_{s3})	0.032				
Disaster vulnerability (w_v)					0.321
Disaster prevention capability (w_p)					0.094

In order to eliminate dimension, all factors in the integrated model were normalized based on two different assumptions, one was the effect of 'the bigger the better' (Eq.8), i.e. for V; another was the effect of 'the smaller the better' (Eq.9), i.e. for H. The normalizing assumption for P and S was as the same as for H.

$$V_i'=0.5+0.5\times\frac{V_i-V_{\min}}{V_{\max}-V_{\min}} \tag{8}$$

$$H_i'=0.5+0.5\times\frac{H_{\max}-H_i}{H_{\max}-H_{\min}} \tag{9}$$

3 RESULTS

3.1 *Hazard*

The flood hazard increased from southwest to northeast in Hainan. High flood hazard distributed in the eastern region(Fig.2a) where big precipitation variability existed and rainstorm occurred frequently.

The chilling hazard increased from south to north. High chilling hazard was located in the north Wuzhishan mountain area of Hainan. Low chilling hazard distributed in eastern and southern border of Hainan (Fig.2b). High chilling in regions north of Wuzhishan was caused by a stationary front generated in the Wuzhishan mountain area in central Hainan when cold air moved in, which caused an interaction between cold air and warm air.

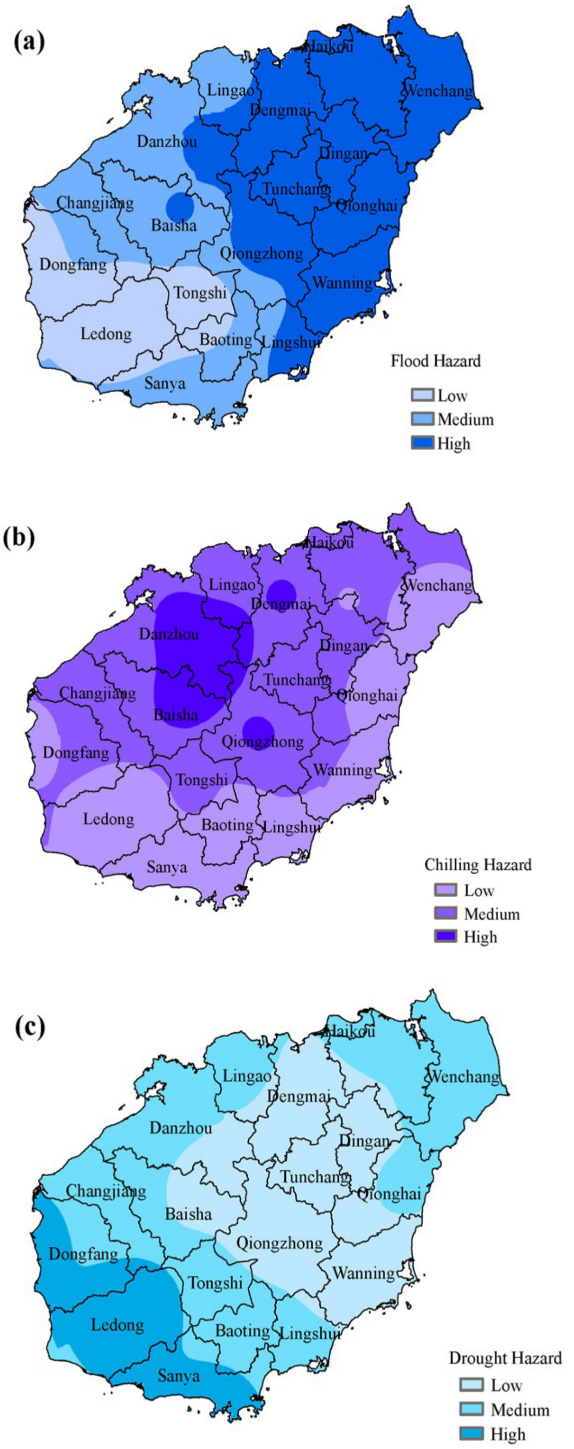

Figure 2. The distribution of disaster hazard in paprika pepper in Hainan.

The drought hazard increased from central to eastern and western Hainan (Fig.2c). High drought hazard was located in western Hainan where less cold air activities and south-west trough were activated. The low drought hazard was in the central part of Hainan.

3.2 *Sensitivity*

The low flood sensitivity was mainly located in central Hainan valley regions around Wuzhishan-Yingeling-Yajiada mountains area (Fig.3a) due to the influence of terrain characteristics prone to water accumulation. The drought sensitivity decreased from the central part with high slope of terrain prone to water running off to coastal plains (Fig.3c). The high chilling sensitivity was distributed in the central mountain area due to the low temperature caused by high altitude(Fig. 3b).

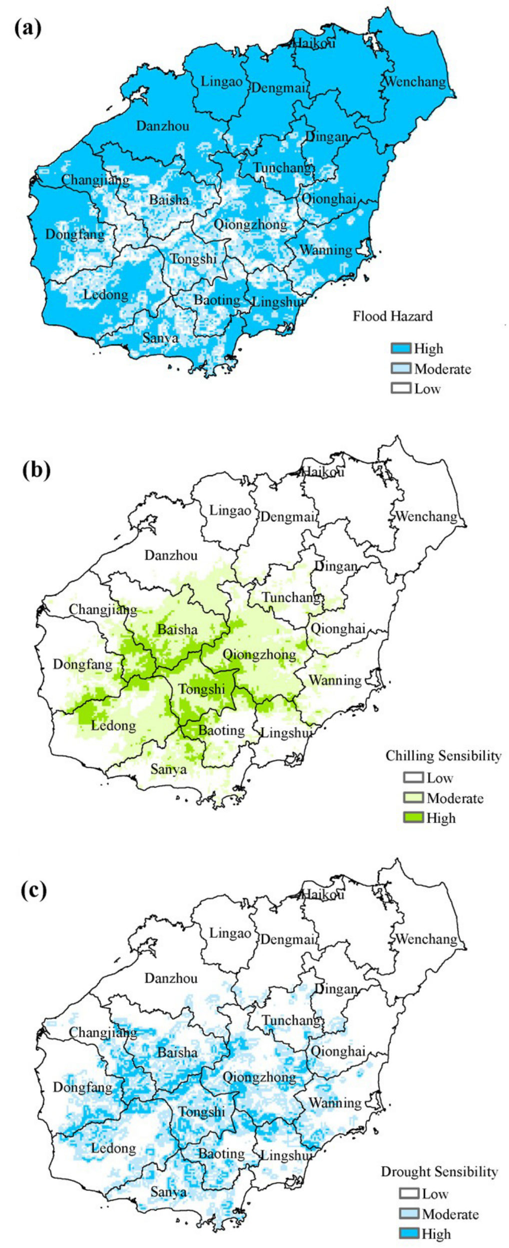

Figure 3. Distribution of the disaster sensitivity in paprika pepper in Hainan.

3.3 *Vulnerability*

High disaster vulnerability (see Fig.4) was mainly located in the central part of southwest regions in Hainan, i.e. Baisha, Tongshi and Haikou city, where average yield losses in paprika pepper caused by overall disasters exceeded 50%. The northeast region of Hainan had a low vulnerability for major disasters, while average yield loss was less than 20%.

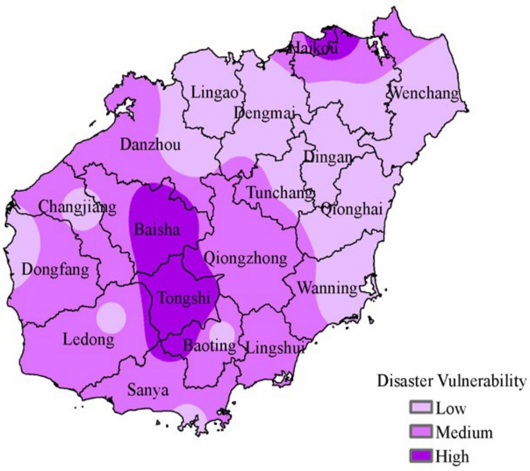

Figure 4. Distribution of the disaster vulnerability in paprika pepper in Hainan.

3.4 *Prevention capability*

Integrating with the five factors, the overall disaster prevention capability (see Fig.5) was high in the east and northwest regions in Hainan where the yearly variation of yields was lower and economic development was higher, compared to the central part.

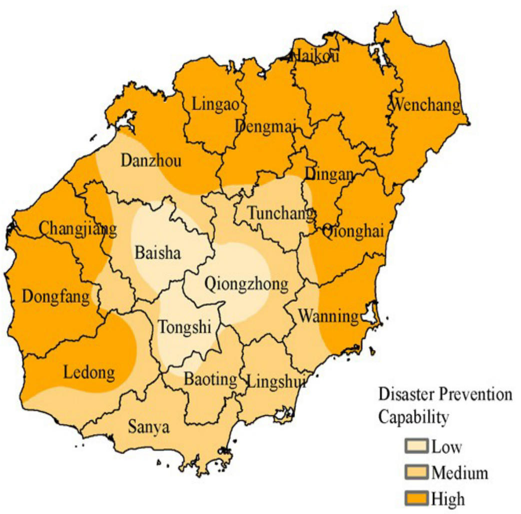

Figure 5. Distribution of the disaster prevention capability for paprika pepper in Hainan.

3.5 *Integrated risk assessment of major disasters*

High integrated disaster risk was mainly distributed in the east region of Hainan, and decreased from east to west. Yield reduction in paprika pepper reached 81.8% due to a low tolerance and high suberification to flood, when the flood was the major factor that caused yield loss during 1999–2011 according to the historical records. Land property and conditions, i.e. hilly, inhomogeneous reservoirs, poorly drained soil and low-quality irrigation systems also provided considerable influences.

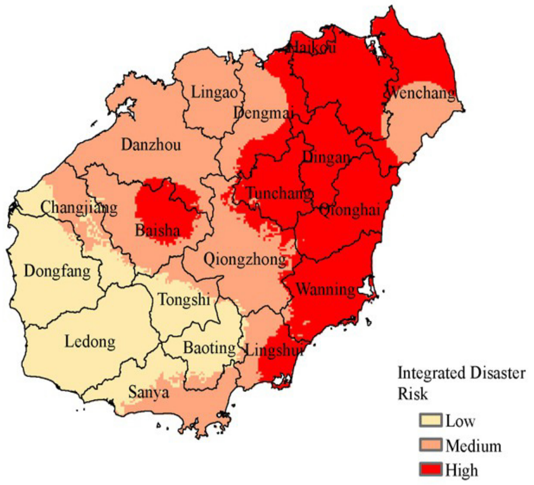

Figure 6. Distribution of integrated risk for major disasters in paprika pepper in Hainan.

4 DISCUSSION AND CONCLUSION

The series indices for assessing hazard, sensitivity, vulnerability and prevention capability of flood, chilling and drought disasters were built based on long-term climatic, topographic, agricultural and economic data. Integrating single indices into a combined disaster risk assessment model, an integrated disaster risk assessment model was developed to quantitatively assess the risk of major disasters (flood, chilling and drought) in paprika pepper in tropical climate. The calculated hazard and risk provided good agreement with actual occurrence of disasters and crop production. Hazard indices for the three disasters were convenient and practical to use in monitoring and taking precaution in paprika pepper production. Knowing the distribution of a single risk index for three major disasters in Hainan could help farmers and policy makers optimize their disaster management.

The hazard of flood was not only caused by precipitation more than 20% above the mean (Fig.7a) but also by over 35 rainy days in east Hainan. The crop water requirement was also an important factor which determined flood, when it was much lower than precipitation during certain periods. For the hazard of drought, except for the precipitation under mean value merely meeting the requirement for paprika pepper in the west parts, average dry days were more than 35 days (Fig.7c) determining high drought damage.

Although the accumulated chilling (with chilling temperature was lower than 12℃) was bigger in central-northern Hainan (Fig.7b), it did not give a good prediction of the typical chilling year 2000 and non-chilling year 2003 while the two years had similar accumulated chilling. It might be caused by the days that completed a chilling event, e.g. five continuous days with chilling temperature below 12℃. The prediction results showed a good agreement with historical records when we introduced a continuous five-day chilling period into the index. It indicates that the chilling damage is not additive during the whole crop growing season, but only accumulated during a short period.

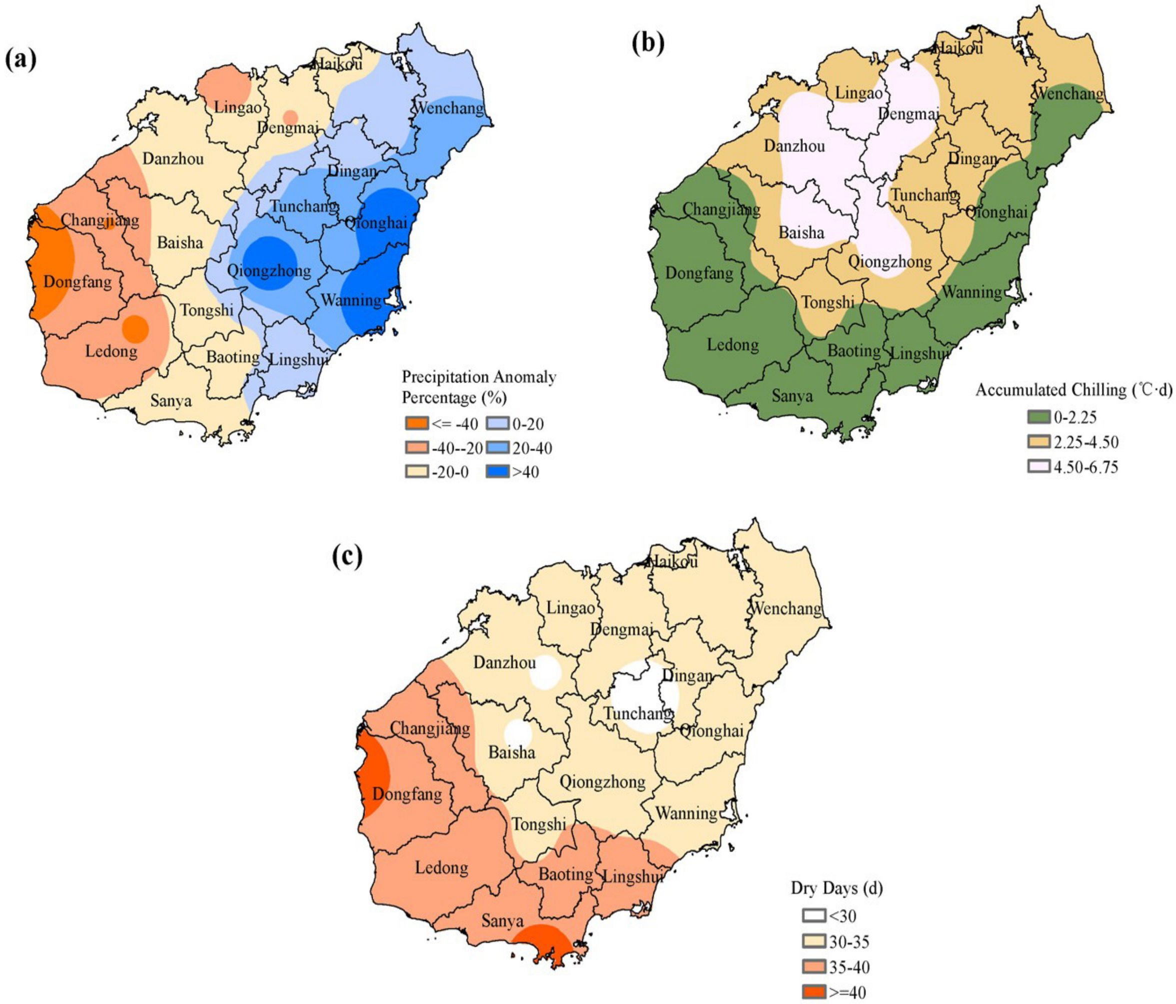

Figure 7. Distribution of climatic characteristics in Hainan.

Uncertainty is a significant component in the hazard risk assessment. During the chilling process, low temperature and rain always concurrently occurred as were induced by the interaction between warm and cold air in Hainan. Besides, flood happened when a large amount of precipitation (Wang et al.[39]) appeared rather than a small amount. One critical threshold value of precipitation might exist in the flood hazard index as well as in the drought hazard index that can be calculated to significantly increase the precision in hazard analysis.

For disaster sensitivity, slope gradient and altitude were considered as the major factors which could reveal formation environment characteristics of major disasters. Disaster-induced elements, i.e. water content and temperature varied on account of regional terrain and topography, which could reflect the variation of sensitivity to disasters on different geological units (Sun et al.[40]; Iyalomhe et al.[41]) and be applied in analysis of similar sensitivity induced by regional terrain. As the consequence of climate and ecosystem, diverse soil texture existed in regions ranging from sand to clay (Qiu et al.[42]), i.e. loam-clay soil mainly in the east part and sand soil in the west part in Hainan. Retention characteristics of water varied in different soil texture which could lead to different disaster sensitivity to precipitation (Zhang et al.[14]). Although it is difficult to quantify the effect of soil texture in disasters, we should take it into account in the future for assessing the sensitivity of disasters, especially for water-induced ones.

Attempts to develop the quantification of vulnerability have progressed ahead with an increasing emphasis on the need to describe the vulnerability of disasters (Kahn[43]; Noriega and Ludwig[44]) based on the accessibility of data on large scales. Vulnerability assessments have been limited by spatial scales and the affected body to be quantified (Jeffers[45]), using the data pertinent to determining the potential for loss. Yield reduction in one specific crop was often regarded as an effective indicator for evaluating the degree of damage caused by meteorological disasters (Zhang et al.[14]). By combination of the yield reduction rate and its risk probability of disasters vulnerability could be calculated relatively easily, which comprehensively reflects the actual damage consequences in paprika pepper induced by major disasters. However this attempt at quantification of vulnerability has also revealed disagreements and the lack of other relevant indicators, like the affected area over total crop sowing area and disasters frequency (Wei et al.[46]), which is necessary to be included in future researches.

In terms of the prevention capability, aggregating available resources were adopted to mitigate the negative effects of disasters damage (Rufat et al.[47]). This aggregating ability could be quantified by the level of social-economic and agricultural factors in a region, which is referred to as an overall prevention capability of disasters for a certain crop. The improvement of hydraulic facility, i.e., irrigation facilities and drainage systems (Sarkar et al.[48]), as well as public policy, i.e., insurance policy (Koks et al.[49]; Jain et al.[50]) to recover from disasters and mitigation measures, had been proven to substantially lower the damage (Hudson et al.[51]). Considering the availability of data sources, the regional information of net income in the rural area and agricultural machinery gross power was easy to obtain from national statistics, which could well reflect the overall ability of the region to prevent and recover from disaster damage.

The developed integrated risk assessment model for major disasters in paprika pepper based on hazard, sensitivity, vulnerability and prevention capability performed well in assessment of natural meteorological disasters in conformity with actual disasters situation in tropical climate. This new model could be flexibly applied for single or multiple disasters not only in paprika pepper but also provide a good tool in other crops around the world. The results provide a scientific base for the improvement of agricultural management and the implementation of disasters prevention and mitigation measures.

Acknowledgement: We extended our gratitude to the editor-in-chief and anonymous reviewers of Journal of Tropical Meteorology for their constructive comments on improving the quality of this paper.

REFERENCES:

[1] Emergency Events Database The OFDA/CRED International Disaster Database [DB]. www.emdat.be-Universite Catholique de Louvain, Brussels, Belgium, 2014.

[2] ZHANG Zhao, WANG Pin, CHEN Yi, et al. Spatial pattern and decadal change of agro-meteorological disasters in the main wheat production area of China during 1991-2009 [J]. J Geogr Sci, 2014, 24(3): 387-396.

[3] JIA Jing-dun, JIANG Zhou-ping, CHEN Liang-yu, et al. China's Agricultural Research Progress and Countermeasures to Cope with Climate Change [M]. Beijing: China Agricultural Science and Technology Press, 2013.

[4] LUEDELING E, GEBAUER J, BUERKERT A. Climate change effects on winter chill for tree crops with chilling requirements on the Arabian Peninsula [J]. Clim Change, 2009, 96(1): 219-237.

[5] AGHDAM M S, MOHAMMADKHANI N. Enhancement of chilling stress tolerance of tomato fruit by postharvest brassinolide treatment [J]. Food Bioprocess Tech, 2014, 7: 909-914.

[6] BI H Q, PAREKH J, Li Y, et al. Adverse influences of drought and temperature extremes on survival of potential tree species for commercial environmental forestry in the dryland areas on the western slopes of New South Wales, Australia [J]. Agr Forest Meteorol, 2014, 197: 188-205.

[7] DEO R C. On meteorological droughts in tropical Paci?c Islands: time-series analysis of observed rainfall using Fiji as a case study [J]. Meteor Appl, 2011, 18(2): 171-180.

[8] VARAZANASHVILI O, TSERETELI N, AMIRANASHVILI A, et al. Vulnerability, hazards and multiple risk assessment for Georgia [J]. Nat Hazards, 2012, 64(3): 2021-2056.

[9] GLADE T, NADIM F. Early warning systems for natural hazards and risks [J]. Nat Hazards, 2014, 70(3): 669-1671.

[10] IPCC. Climate change 2014: Impacts, adaptation and vulnerability [R]. Working group II contribution to the fifth assessment report of the intergovernmental panel on climate change, Yokohama, Japan, March, 2014.

[11] PETR M, BOERBOOM L G J, VEEN A V D, et al. A spatial and temporal drought risk assessment of three major tree species in Britain using probabilistic climate change projections [J]. Clim Change, 2014, 124: 791-803.

[12] DELIN S, BERGLUND K. Management zones classified with respect to drought and waterlogging [J]. Precis Agric, 2005, 6(4): 321-340.

[13] QUAN R S, LIU M, LU M, et al. Waterlogging risk assessment based on land use/cover change: a case study in Pudong New Area, Shanghai [J]. Environ Earth Sc, 2010, 61: 1113-1121.

[14] ZHANG J Q. Risk assessment of drought disaster in the maize-growing region of Songliao plain, China [J]. Agr Ecosyst Environ, 2004, 102: 133-153.

[15] XU X C, GE Q S, ZHEN J Y. Agricultural drought risk analysis based on three main crops in prefecture-level cities in the monsoon region of east China [J]. Nat Hazards, 2013, 66(2): 1257-1272.

[16] TODISCO F, MANNOCCHI F, VERGNI L. Severity-duration-frequency curves in the mitigation of

drought impact: an agricultural case study [J]. Nat Hazards, 2013, 65(3): 1863-1881.
[17] YU X Y, HE X Y, ZHENG H F. Spatial and temporal analysis of drought risk during the crop-growing season over northeast China [J]. Nat Hazards, 2014, 71 (1): 275-289.
[18] DASH B K, RAFIUDDIN M, KHANAM F, et al. Characteristics of meteorological drought in Bangladesh [J]. Nat Hazards, 2012, 64(2): 1461-1474.
[19] POTOPOVA V, STEPANEK P, MOZNY M, et al. Performance of the standardized precipitation evapotranspiration index at various lags for agricultural drought risk assessment in the Czech Republic [J]. Agr Forest Meteor, 2015, 202: 26-38.
[20] TSAKIRIS G, PANGALOU D, VANGELIS H. Regional drought assessment based on the reconnaissance drought index (RDI) [J]. Water Resour Manag, 2007, 21: 821-833.
[21] SHAHID S, BEHRAWAN H. Drought risk assessment in the western part of Bangladesh [J]. Nat Hazards, 2008, 46: 391-413.
[22] LI Yun-jie, REN Fu-min, LI Yi-ping, et al. Characteristics of the regional meteorological drought events in southwest China during 1960-2010 [J]. J Meteor Res, 2014, 28: 381-392.
[23] VERA P, PETR S, MARTIN M, et al. Performance of the standardized precipitation evapotranspiration index at various lags for agricultural drought risk assessment in the Czech Republic [J]. Agr Forest Meteor, 2015, 202: 26-38.
[24] LIU Shi-ye, TAN Zong-kun, BAO Hui-chang. Impacts of low temperature in winter on banana production and yield losing evaluation in Guangxi province [J]. J Meteor Res Appl, 2012, 33: 38-42.
[25] MEGIAS Z, MARTINEZ C, MANZANO S, et al. Cold-induced ethylene in relation to chilling injury and chilling sensitivity in the non-climacteric fruit of Zucchini (Cucurbita pepo L.) [J]. LWT-Food Sci Technol, 2014, 54: 194-199.
[26] REBECCA D, REBECCA W, IAN G, et al. Winter chilling trends for deciduous fruit trees in Australia [J]. Agr Forest Meteor, 2011, 151: 1074-1085.
[27] GIULIA V, GIULIA H, MARTIN W. Snowed in for survival: quantifying the risk of winter damage to overwintering field crops in northern temperate latitudes [J]. Agr Forest Meteor, 2014, 197: 65-75.
[28] CHENG Yong-xiang, HUANG Jing-feng, HAN Zhou-ling, et al. Cold damage risk assessment of double cropping rice in Hunan, China [J]. J Integr Agr, 2013, 12 (2): 352-363.
[29] BELAL A A, RAMADY H R E, MOHAMED E S, et al. Drought risk assessment using remote sensing and GIS techniques [J]. Arba J Geosci, 2014, 7: 35-53.
[30] SANJAY K, RAVISH K, AJANTA G, et al. Application of meteorological and vegetation indices for evaluation of drought impact: a case study for Rajasthan, India [J]. Nat Hazards, 2010, 54(3): 643-656.
[31] WEN Ke-gang, WU Yan-jun. Chinese meteorological disasters ceremony [M]. Beijing: Meteorological Press, 2009.
[32] MASOOD M, TAKEUCHI K. Assessment of flood hazard, vulnerability and risk of mid-eastern Dhaka using DEM and 1D hydrodynamic model [J]. Nat Hazards, 2012, 61: 757-770.
[33] CHENG Zhi-hui. Vegetable cultivation [M]. Beijing: Science Press, 2010.
[34] WU Mei-hua, CHEN Ya-ning, XU Chang-chu. Assessment of meteorological disasters based on information diffusion theory in Xinjiang, Northwest China [J]. J Geogr Sci, 2015, 25: 69-84.
[35] OZSAHIN E, KAYMAZ C K. Avalanche susceptibility and risk analysis of Eastern Anatolian region using GIS [J]. Procedia Soc Behav Sci, 2014, 120: 663-672.
[36] RUIZ V, PEREZ M A, OLASOLO A. Dynamic portfolio panagement ptrategies based on the use of moving averages [J]. Procedia Soc Behav Sci, 2014, 109: 1277-1281.
[37] NASIRI H, BOLOORANI A D, SABOKBAR H A F, et al. Determining the most suitable areas for artificial groundwater recharge via an integrated PROMETHEE II-AHP method in GIS environment (case study: Garabaygan Basin, Iran) [J]. Environ Monit Assess, 2013, 185: 707-718.
[38] BENEDETTO F, GIUNTA G, MASTROENI L. A maximum entropy method to assess the predictability of financial and commodity prices [J]. Digit Signal Process, 2015, 46: 19-31.
[39] WANG Yan-jun, GAO Chao, ZHAI Jian-qing, et al. Spatio-temporal changes of exposure and vulnerability to ?oods in China [J]. Adv Climate Change Res, 2014, 5: 197-205.
[40] SUN L Y, WANG S Y, LU H, et al. Simulations of configurational and granular temperatures of particles using DEM in roller conveyor [J]. Powder Technol, 2014, 268: 436-445.
[41] IYALOMHE F, RIZZI J, PASINI S, et al. Regional Risk Assessment for climate change impacts on coastal aquifers [J]. Sci Total Environ, 2015, 537: 100-114.
[42] QIU Peng-hua, XU Song-jun, XIE Gen-zong, et al. Analysis of the ecological vulnerability of the western Hainan Island based on its landscape pattern and ecosystem sensitivity [J]. Acta Ecol Sinica, 2007, 27(4): 1527-1264.
[43] KAHN S. Vulnerability assessments and their planning implications: a case study of the Hutt Valley, New Zealand [J]. Nat Hazards, 2012, 64: 1587-1607.
[44] NORIEGA G., LUDWIG L. Social vulnerability assessment for mitigation of local earthquake risk in Los Angeles County [J]. Nat Hazards, 2012, 64 (2): 1321-1355.
[45] JEFFERS J M. Integrating vulnerability analysis and risk assessment in flood loss mitigation: An evaluation of barriers and challenges based on evidence from Ireland [J]. Appl Geogr, 2013, 37: 44-51.
[46] WEI Y M, FAN Y, LU C, et al. The assessment of vulnerability to natural disasters in China by using the DEA method [J]. Environ Impact Asses, 2004, 24: 427-439.
[47] RUFAT S, TATE E, BURTON C G, et al. Social vulnerability to floods: Review of case studies and implications for measurement [J]. Int J Disaster Risk Reduct, 2015, 14: 470-486.
[48] SARKAR S, PARIHAR S M, DUTTA A. Fuzzy risk assessment modelling of East Kolkata Wetland Area: A

remote sensing and GIS based approach [J]. Environ Modell Softw, 2016, 75: 105-118.
[49] KOKS E E, JONGMAN B, HUSBY T G. Combining hazard, exposure and social vulnerability to provide lessons for flood risk management [J]. Environ Sci Policy, 2015, 47: 42-52.
[50] JAIN G. The role of private sector for reducing disaster risk in large scale infrastructure and real estate development: Case of Delhi [J]. Int J Disaster Risk Reduct, 2015, 14: 238-255.
[51] HUSDON P, BOTZEN, W J W, KREIBICH H. Evaluating the effectiveness of flood damage mitigation measures by the application of propensity score matching [J]. Nat Hazard Earth Syst Sci Discuss, 2014, 2 (1): 681-723.

Citation: ZHANG Lei, HUO Zhi-guo, ZHANG Li-zhen et al. Integrated risk assessment of major meteorological disasters with paprika pepper in Hainan province [J]. J Trop Meteor, 2017, 23(3): 334-344.